Effects of He Plasma Pretreatment on Low-k Damage during Cu Surface Cleaning with NH3 Plasma

ARTICLE *in* JOURNAL OF THE ELECTROCHEMICAL SOCIETY · JANUARY 2010

Impact Factor: 3.27 · DOI: 10.1149/1.3355881

6 AUTHORS, INCLUDING:

Adam Michal Urbanowicz
Nova Measuring Instruments
37 PUBLICATIONS **304** CITATIONS
SEE PROFILE

Alban Zaka
GlobalFoundries Inc.
25 PUBLICATIONS **93** CITATIONS
SEE PROFILE

Stefan De Gendt
imec Belgium
530 PUBLICATIONS **4,916** CITATIONS
SEE PROFILE

Mikhail R Baklanov
imec Belgium
354 PUBLICATIONS **4,505** CITATIONS
SEE PROFILE

Journal of The Electrochemical Society, **157** (5) H565-H573 (2010)
0013-4651/2010/157(5)/H565/9/$28.00 © The Electrochemical Society

Effects of He Plasma Pretreatment on Low-*k* Damage during Cu Surface Cleaning with NH_3 Plasma

A. M. Urbanowicz,[a,b,*,z] D. Shamiryan,[a] A. Zaka,[a,c] P. Verdonck,[a] S. De Gendt,[a,b,] and M. R. Baklanov[a]**

[a] *IMEC, Leuven, Belgium B3001*
[b] *Chemistry Department, Katholieke Universiteit Leuven, Leuven, Belgium B3001*
[c] *Materials Engineering Department, Institut National des Sciences Appliquées de Lyon, Villeurbanne, France 69621*

In this study, the effect of the sequential He and NH_3 plasma treatments on a chemical vapor deposition SiOC:H low-*k* dielectric is evaluated in the wide range of experimental conditions. Results show that the active NH_3 plasma radicals penetrate the porous low-*k* bulk and remove the hydrophobic Si–CH_3 groups, which leads to hydrophilization and results in the degradation of dielectric properties. The implementation of He plasma pretreatment reduces the damage imposed by the NH_3 plasma by a stimulation of the surface recombination of active radicals from NH_3 plasma. He plasma causes a surface modification of 10–20 nm presumably due to the energy transfer from the extreme UV photons and the 2^1S He metastable atoms to the low-*k* structure. The plasma damage reduction is proportional to He plasma density and the treatment time. The mechanism of plasma damage reduction is explained on the basis of the Knudsen diffusion mechanism and random walk theory.
 [DOI: 10.1149/1.3355881]

Manuscript submitted January 12, 2009; revised manuscript received January 6, 2010. Published April 7, 2010.

The integration of porous low dielectric constant (low-*k*) materials is a persistent issue in microelectronics industry.[1] One of the most difficult challenges is related to the high sensitivity of porous materials to chemicals and plasmas. Pores and their connectivity significantly increase the penetration depth of active species during different technological processes such as plasma etching and cleaning, deposition of barrier layers, and chemical mechanical polishing (CMP).[2] The most severe damage of low-*k* materials occurs during their exposure to strip/cleaning plasmas containing oxygen or a mixture of nitrogen and hydrogen. The active radicals formed in these plasmas are able to remove carbon-containing hydrophobic groups with the formation of volatile compounds such as CO, CO_2, H_2O, and CH_4. The formation of these compounds is thermodynamically favorable. As a result of the carbon depletion, the films become hydrophilic.[1,3] Subsequent moisture absorption in the pores significantly increases the *k*-value due to the high polarizability of water molecules. All these phenomena have been extensively studied and documented for the resist strip and post-dry-etch cleaning.[4] However, some additional issues are related to the cleaning of the Cu/low-*k* stack after planarization by CMP. The purpose of the post-CMP cleaning is the reduction of Cu oxide on the Cu surface. Therefore, only reducing plasmas can be used for this purpose. NH_3 plasma treatment is a popular approach because this plasma enables both the reduction of Cu oxides without deterioration of the adhesion with the subsequent dielectric liner and the removal of residual particles.[5,6] However, NH_3 plasma treatment leads to a significant modification of the chemical composition and degradation of low-*k* films (carbon depletion and subsequent hydrophilization). This degradation is related to the penetration of active radicals from NH_3 plasma into porous low-*k* materials. Therefore, low-*k* materials with porosity larger than 20% require process optimization with respect to plasma damage.

One of the effective strategies to reduce bulk low-*k* damage is surface activation to trap the radicals at the surface. The reduction of O and NO_2 plasma damage by using He plasma pretreatment in a plasma-enhanced chemical vapor deposition (PECVD) chamber were reported by Wang et al.[7] and Yanai et al.,[8] respectively. However, the mechanism of plasma damage reduction was not discussed. Authors reported[4,5,9] that the preliminary exposure of the low-*k* surface to He plasma makes it more resistant to NH_3 plasma and proposed the mechanism of plasma damage reduction. The extreme ultraviolet (EUV) emission from He plasma creates chemically active sites and decreases pore radii on the low-*k* surface, which leads to the recombination of active radicals on the surface. In certain cases, the activated surface could stimulate and localize chemical reactions, providing sealing of low-*k* materials. In this work, we discuss the effect of the NH_3 plasma on the low-*k* dielectric and the effect of He plasma pretreatments at different radio-frequency (rf) powers and exposure times on the NH_3 plasma damage resistance of the low-*k* dielectric. We demonstrate, in addition to our previous work,[9] that the low-*k* bulk damage reduction in the sequential plasma He + NH_3 treatments is proportional to He plasma density. Furthermore, we discuss a model to describe key parameters for the plasma damage reduction in the sequential He + NH_3 treatment on the basis of the Knudsen diffusion mechanism and random walk theory. Finally, we show that differential Fourier transform IR (FTIR) spectroscopy can be used to monitor the pore sealing efficiency in the sequential He + NH_3 plasma treatment.

Experimental

Dielectric material.— Porogen-based Aurora® ELK (extreme low-k) HM (high modulus) low-*k* films from the American Society of Metals (ASM) with a *k* value of 2.5 were used for the experiments.[10] Approximately 180 nm thick films were deposited on 300 mm Si wafers by PECVD. The porosity of the deposited low-*k* films was typically close to 25% with a mean pore radius of 0.7 nm, measured by ellipsometric porosimetry (EP).[11,12]

Plasma treatment conditions.— All experiments were carried out in the Eagle 12 plasma chamber from ASM. This reactor is a capacitive-coupled plasma (CCP) system. Using an rf of 13.56 MHz, the rf power was varied from 400 to 1400 W. The effect of ion bombardment was minimized because a wafer sat on a grounded electrode. The wafer temperature was approximately 350°C. For the damage evaluation, blanket low-*k* films were exposed to NH_3, He, and successive He and NH_3 plasma treatments. The experimental conditions are summarized in Table I. The effect of the NH_3 plasma was evaluated after the exposure of low-*k* samples to 900 W NH_3 plasma for 15 s at a gas pressure of 530 Pa and a gas flow of 400 sccm.

Successive He + NH_3 plasma treatments.— He plasma exposure was followed by the NH_3 plasma exposure. The NH_3 plasma treatment was the same for all experiments (as described above). All the He pretreatments were performed using the same gas pressure of 630 Pa and gas flow of 1000 sccm. Two parameters of He plasma

* Electrochemical Society Student Member.
** Electrochemical Society Active Member.
z E-mail: urbano@imec.be

Table I. Summary of experimental conditions.

Parameter	He plasma pretreatment	NH_3 plasma treatment
Time (s)	0–60	0–15
Pressure (Pa)	630	530
RF power (W)	400–1400	900
He flow (sccm)	1000	0
NH_3 flow (sccm)	0	400

were varied for successive He + NH_3 plasma treatments: rf power (400, 600, 800, and 1400 W) using the constant time of 20 s and time (20, 40, and 60 s) with a constant rf power of 1400 W. Furthermore, we used 600 W of rf power for 60 s. This additional experiment was done to evaluate the influence of rf power on the surface sealing of the low-*k* material.

He plasma treatments.— To study the effect of He plasmas, we first used 400 and 800 W of rf power and a constant time of 20 s. Furthermore, 1400 W He plasma with times of 40 and 60 s and, additionally, 60 s of 600 W plasma treatments were used.

Metrology.— The thickness and refractive index of reference and plasma-treated films were measured by a SENTECH 801 spectroscopic ellipsometer (SE) mounted onto a vacuum chamber. The measurements under vacuum allow us to eliminate the effect of adsorbed moisture on the optical properties of the hydrophilic films. The spectra were recorded in the wavelength range of 350–850 nm. Optical properties and thickness were determined by fitting models to the measured spectra of the ellipsometric polarization angles at 70° by single- and double layer optical models using the Marquardt–Levenberg algorithm. The film thickness was estimated using a double layer SE model based on the Cauchy approximation. The bottom layer was assumed to have optical properties of the as-deposited film, while the optical characteristics of the top modified layer were determined by fitting. The open porosity, pore size distributions, and surface sealing effects (i.e., top surface densification by plasma treatment) of the low-*k* films were evaluated by toluene-based EP [11,12] using the ellipsometric system coupled with vacuum chamber, as described above. EP used in situ ellipsometry to determine the amount of the adsorptive (i.e., toluene), which was adsorbed/condensed in the film. A change in the refractive index caused by toluene was used to calculate the quantity of toluene present in the film. The volume fraction filled with toluene at saturation vapor pressure (SVP) determined the open porosity of the low-*k* film. The pore size distribution was calculated using toluene desorption isotherms.[11] EP was also used to evaluate surface sealing effects caused by plasma modifications of the porous low-*k* film.[13-15] The surface sealing effect appeared when the pore neck size at the top surface decreased, which resulted in the decrease in the toluene diffusion rate through the densified surface layer. This was reflected in the delay between the toluene adsorption and desorption isotherms. The full surface sealing effect appeared when the toluene absorption was not observed. In this case, the pore neck size was comparable with the toluene molecule size (6 Å).

The hydrophilization of low-*k* materials was characterized by three methods. The first one was water-based EP.[16] This method was sensitive to the bulk hydrophilicity of low-*k* films. The volume fraction of the porous low-*k* film filled with water at SVP reflected the degree of the hydrophilization of the porous film bulk. The second method was water-based goniometry that measures water contact angle (WCA) with the film surface. The WCA reflected the hydrophobic properties of the film surface. The third method was FTIR spectroscopy to study the integrated absorbance of –OH and H_2O groups.

The molecular bands of low-*k* films before and after plasma treatments were analyzed using FTIR spectroscopy (Biorad QS2200 ME). The spectra were recorded in the range of 4400–400 cm^{-1} in nitrogen ambient. The nitrogen ambient was applied to reduce absorbance from ambient such as moisture and CO_2. In certain cases, the spectrum before the plasma treatment was subtracted from the spectrum after the treatment. The obtained differential spectra reflected the difference in absorbance between the as-deposited and the plasma-damaged film and allowed us to analyze the small modifications that were not pronounced in normal spectra.

Time-of-flight secondary-ion mass spectroscopy (TOF-SIMS) was used to obtain the concentration profile of the film components. The data were obtained using an IONTOF IV instrument in a noninterlaced dual beam mode with a Xe sputtering beam and a bunched 15 keV Ga analysis beam to detect negative secondary ions. The Ga analysis beam was rastered over a 100 × 100 μm area. The Xe sputtering beam was used with 1 keV of impact energy and 80 nA of current using a raster size of 500 × 500 μm.

Results

Effect of power and time of He pretreatment.— Structural modification.— The reduction in the concentration of organic hydrophobic agents (carbon depletion) is one of the measures of plasma damage. The depth of carbon depletion as measured by TOF-SIMS is shown in Fig. 1. The pure He plasma causes minimal C-depletion, while the NH_3 plasma produces the highest C-depletion. The degree of C-depletion is strongly reduced by a He plasma treatment preceding the exposure to the NH_3 plasma. This effect becomes more pronounced at higher rf power levels of He plasma pretreatment. The depth of the C-depletion is twice as low after the combined 1400 W He + NH_3 plasma when compared with the pure NH_3 plasma treatment.

The bonding structure of the low-*k* material was studied by FTIR. The amount of Si–CH_3 groups is expressed as a ratio of integrated absorbance of Si–O (970–1260 cm^{-1}) and Si–CH_3 (1260–1290 cm^{-1}) groups, as shown in Fig. 2. The reduction of Si–CH_3/Si–O ratio indicates the removal of Si–CH_3 groups. The dotted line represents the Si–CH_3/Si–O ratio of the as-deposited film (reference level). The removal of the Si–CH_3 groups is observed after each plasma treatment, but the biggest C-depletion occurs after NH_3 only and 400 W He + NH_3 plasma treatments. FTIR data (Fig. 2a) support previous conclusions based on TOF-SIMS results that the minimal C-depletion occurs in He plasma, and the degree of depletion is reduced by the combination of He and NH_3 plasma treatments starting from a He rf power of 600 W.

Figure 2b represents the Si–CH_3/Si–O ratio vs time of He plasma treatment. The Si–CH_3 bond depletion is limited for combined He + NH_3 plasma treatments and decreases with time of He pretreatment. For a constant time of 60 s, the higher power of He

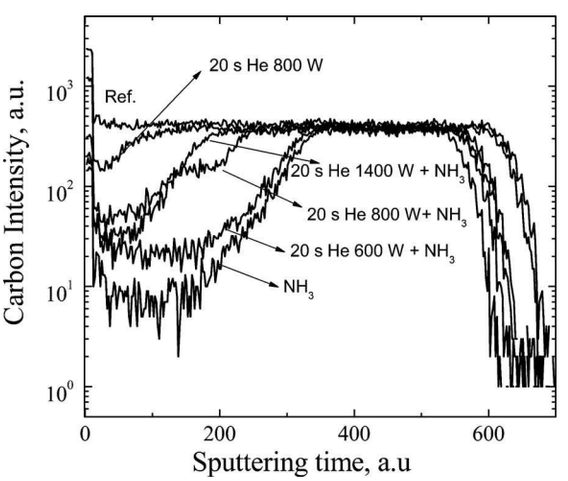

Figure 1. Carbon depth profile of the as-deposited and plasma treated films as measured by TOF-SIMS.

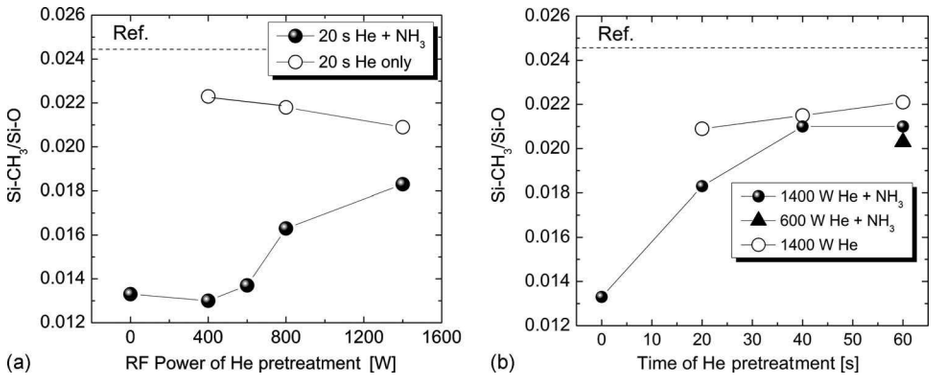

Figure 2. (a) The ratio of integrated absorbance of Si–CH_3 and Si–O (as measured by FTIR) vs rf power of He pretreatment. (b) The ratio of integrated absorbance of Si–CH_3 and Si–O (as measured by FTIR) vs time of He pretreatment.

pretreatment (1400 W) results in a more effective reduction of the Si–CH_3 bond depletion. Figure 3 shows open porosity as measured by the toluene-based EP. The pristine low-*k* film has 25% of open porosity. The open porosity increases slightly by 1–2% after the NH_3 plasma treatment. On the contrary, the pure He plasma treatment reduces the open porosity by 3–4%.

Increasing the rf power (starting from 600 W) of 20 s He pretreatment inhibits the effect of porosity increase imposed by the NH_3 plasma. However, we did not find any evidence of surface sealing effect. The adsorption and desorption isotherms followed the same trend, as in the pristine material. In contrast, longer exposure times (40 and 60 s) of He plasma with a maximal power of 1400 W in the combined He + NH_3 treatments caused the surface sealing effect, as shown in Fig. 4b and 5.

The hysteresis loop between adsorption and desorption branches of the isotherms is related to a delay in the pore filling and emptying during the adsorption and desorption cycles (Fig. 4b). The integral refractive index measured in vacuum increases slightly from 1.367 for a reference sample to 1.382 after the 60 s He + 15 s NH_3 plasma treatment. This suggests that the total porosity changes insignificantly, and, therefore, the bulk of the film is still porous. Therefore, the diffusion limitation of the toluene penetration is only related to the densification of the top part of the film. Such "partial sealing" indicates a decrease in size of the pore necks at the surface. In this case, it is not possible to calculate the pore size distribution. We can only conclude that the effective pore size in the top part of the film becomes comparable with the size of toluene molecules, approximately 6 Å.

Quantification of the sealing efficiency can be based on the "delay" between the toluene adsorption and desorption branches $\tau/2$ vs time of the plasma treatment. The $\tau/2$ is the difference between the values of P/Po on the adsorption and desorption curves that correspond to the pore filling of 50%, as indicated by an arrow in Fig. 4b. In all these experiments, the rate of the pressure change was the same. Therefore, this delay reflects the change in the toluene diffusion rate through the top densified layer. A longer delay corresponds to a smaller size of the remaining pores. The $\tau/2$ increases with the time of He plasma treatment, as shown in Fig. 5. Therefore, the degree of densification of the top densified layer depends on the

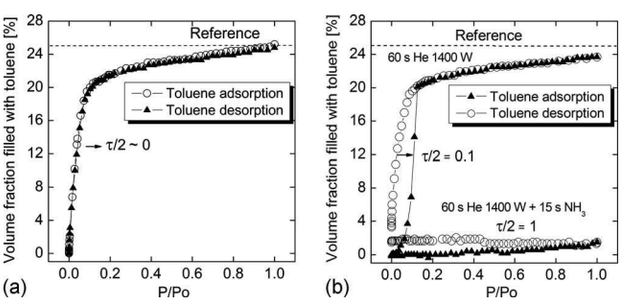

Figure 4. (a) Toluene adsorption/desorption isotherms (as measured by toluene-based EP) for as-deposited low-*k* film (reference). (b) Toluene adsorption/desorption isotherms (as measured by toluene-based EP) for low-*k* films after 60 s of He plasma treatment and subsequent 60 s He + 15 s NH_3 plasma treatment.

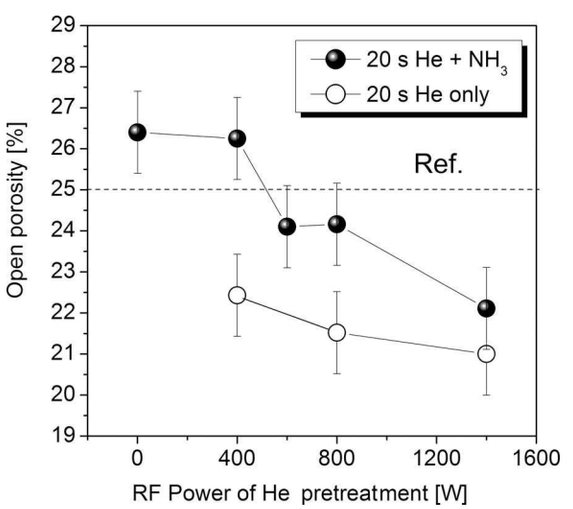

Figure 3. Open porosity (as measured by EP) vs rf power of He pretreatment.

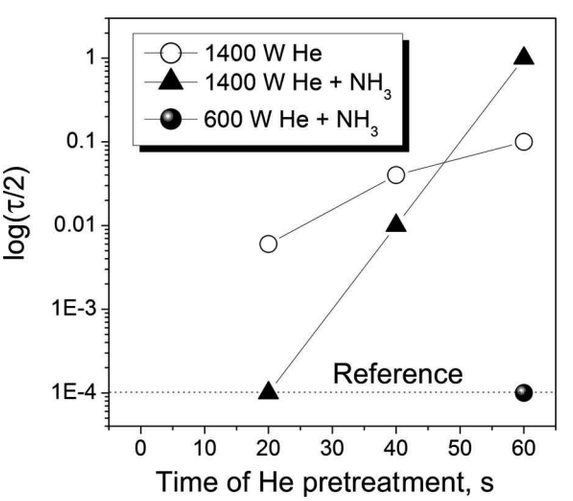

Figure 5. Delay between adsorption and desorption isotherms of toluene (calculated from EP data) for different times of plasma treatment.

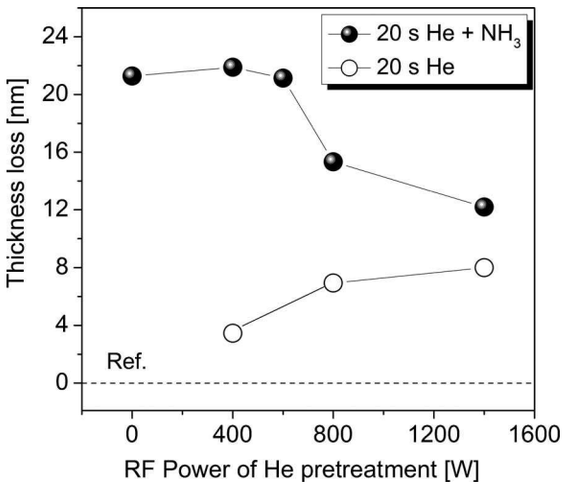

Figure 6. The thickness loss as measured by visible (VIS) (in the range 350 nm-780 nm) SE.

time of He plasma treatment. The porous low-*k* film after subsequent 60 s He and NH_3 plasma treatment does not show any toluene adsorption (Fig. 4b). This proves that the pore size approaches the toluene molecule size of 6 Å (surface sealing effect).

The surface sealing effects can also be studied using the EP system and analyzing a solvent filling time at the solvent SVP.[14] The solvent penetration increases with the filling time dependent on the barrier integrity (surface sealing efficiency).[14,15] To study this, the fully sealed sample treated with 60 s He + 15 NH_3 plasma was filled with toluene for approximately 3000 s. The toluene vapor pressure was increased from 0 to 24 Torr (toluene SVP) in 2000 s. Next, a 1000 s sample was kept in a vacuum chamber at a toluene pressure of 24 Torr. After 1000 s, the change in refractive index was less than 0.003. This shows that after this time, the diffusivity of toluene through the densified layer was close to 0.

The thickness loss after all plasma treatments was measured by SE (Fig. 6). The thickness was extracted from the best fits of a Cauchy model, as discussed in the Metrology section. The NH_3 plasma reduces the thickness of the low-*k* film by about 20 nm. On the contrary, the thickness loss for the pure He plasma treatment is smaller than 8 nm. The thickness loss after NH_3 plasma is reduced in the He pretreatment with an rf power higher than 600 W.

Hydrophobic properties.— Figure 7 shows the amount of adsorbed water measured by water EP for different (a) rf powers and (b) times of He plasma pretreatments. The dotted line represents the water adsorption in a pristine film (1.6%). After 15 s of NH_3 plasma treatment, the amount of adsorbed water increased up to 16%. Comparing this value with the total open porosity (24%), one can conclude that more than 50% of the film becomes hydrophilic. The pure He plasmas of 400 and 800 W almost do not change the hydrophilicity of the film bulk. Pretreatments in He plasmas reduce the degree of bulk hydrophilization imposed by the NH_3 plasma. This reduction is proportional to the rf power of the (a) He plasma and (b) time of the plasma treatment. The treatment of the 1400 W He + NH_3 plasma results in 5.5% of adsorbed water. The combined treatment of the 60 s He 1400 W + 15 s NH_3 plasma results in hydrophilization of 1.6%, which is equal to the as-deposited sample (Fig. 7b). The WCA of the as-deposited film is 95°. The reduction in the CAW is observed after all treatments. However, it was possible to distinguish two groups: only He plasma and all treatments containing NH_3. For pure He, the WCA was higher than 20°. For all NH_3-containing treatments, the WCA was lower than that after He plasma only. Therefore, contrary to the bulk properties, the low-*k* surface becomes hydrophilic after all the plasma treatments.

Figure 8a shows the integrated absorbance of –OH groups (3100–3800 cm^{-1}) obtained by FTIR. The hydrophilization is proportional to the amplitude of the Si–OH absorbance band. The dotted line represents the reference data for the as-deposited film. The reference films reveal the –OH absorbance close to 0. He plasma treatment increases the –OH amount. This increase, however, is smaller than that for all NH_3-containing treatments. The pure NH_3 plasma treatment resulted in the highest –OH incorporation. The He pretreatment reduced –OH group incorporation imposed by the pure NH_3 plasma. This reduction was proportional to the rf power of He plasma.

The FTIR spectra of some samples in the spectral range of 600–4000 m^{-1} are shown in Fig. 8b. The investigated low-*k* is characterized by the Si–O–Si backbone (1000–1200 cm^{-1}), Si–CH_3 (1274 cm^{-1}), and Si–H (2250 and 890 cm^{-1}) bonds. The appearance of the absorbance of the Si–OH and H_2O groups (3900–3100 cm^{-1}) depends on hydrophobic properties of the film. The intensities of the Si–CH_3 and Si–H absorbences are decreased after plasma treatments, while the absorbencies of the Si–OH groups are increased. The decrease in Si–CH_3 and Si–H bonds and the increase in Si–OH after He and combined He + NH_3 plasmas are relatively small compared with the pure NH_3 plasma chemistry. The absorbance of the Si–OH groups increases the most after NH_3 due to the significant film hydrophilization and subsequent moisture absorption.

Discussion

The presented experimental data demonstrated that a pure NH_3 plasma produces significant damage to the low-*k* material. Structural and chemical modification of the bulk of the low-*k* material is minimal in pure He plasmas. The He plasma pretreatment before exposure to NH_3 plasma has beneficial effects, such as reduction in plasma damage and possibility of sealing of the low-*k* surface. The

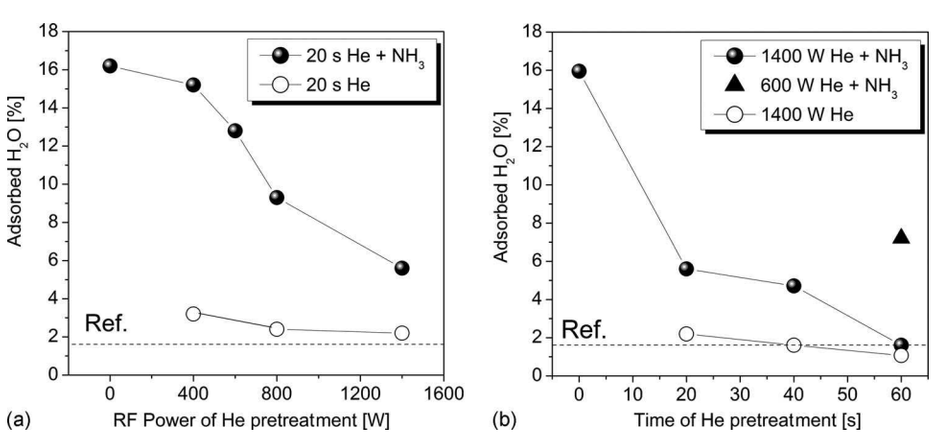

Figure 7. (a) The amount of adsorbed water (as measured by water-based EP) of as-deposited He-plasma-treated and He + NH_3-plasma-treated low-*k* films vs rf power during He plasma treatment. (b) The amount of adsorbed water (as measured by water-based EP) of as-deposited He-plasma-treated and He + NH_3-plasma-treated low-*k* films vs treatment time.

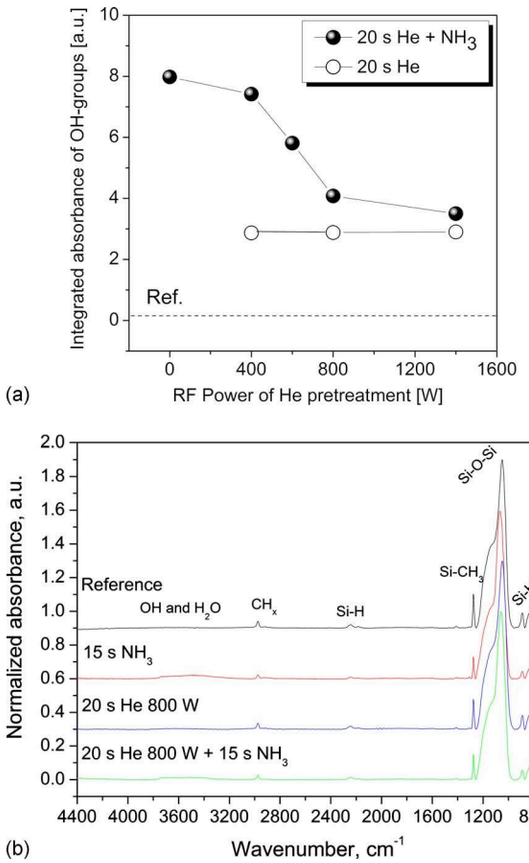

Figure 8. (Color online) (a) Integrated absorbance of OH groups as measured by FTIR vs rf power of He plasma pretreatment. (b) IR absorption spectra of chosen low-*k* films in the range of 4000–400 cm^{-1} as measured by FTIR.

sealing efficiency depends on the time and power of He plasma pretreatment. In the following section, we analyze the nature of the observed phenomena.

Effect of NH_3 plasma.— The most important active components formed in NH_3 plasma are NH_2, N_2H_4, and H radicals. Hydrogen radicals play a key role in the Cu oxide reduction during the post-CMP cleaning. However, all these radicals are chemically active with respect to SiOC:H-based low-*k* materials and result in their damage. The different effects of the NH_3 plasma have already been discussed in addition to the papers reporting damage of the low-*k* materials.[4,9,17,18] Peng et al.[18] reported that NH_3 plasma in certain conditions is able to seal the surface of the MSQ-based low-*k* film. We also showed in our previous work with different types of chemical vapor deposition (CVD) low-*k* materials that pure NH_3 plasma damages the low-*k* material, but the consecutive treatment by He and NH_3 plasmas is able to reduce the plasma damage and seal the surface.[9]

The effect of H radicals on SiOC:H low-*k* films has been extensively studied and well documented[3,4,19-24] because of the wide application of the hydrogen-based plasmas for the resist strip and post-dry-etch cleaning. However, the H_2-based plasmas cause many different effects. Some groups report that these plasmas have no effect on the SiOC:H film,[4,19,20,22] others report that it enhances the dielectric properties,[24] and yet others indicate that H_2 plasmas cause significant damage.[3,21]

The replacement of CH_3 groups by H atoms with a formation of less stable Si–H groups and the breakage of Si–O–Si groups with a formation of hydrophilic silanol groups are thermodynamically favorable[3]

$$\equiv Si\text{–}CH_3 + 2H \rightarrow \equiv Si\text{–}H + \uparrow CH_4$$
$$(\Delta Hr = -411\ kJ\ mol^{-1}\ at\ 298\ K)$$

$$\equiv Si\text{–}O\text{–}Si \equiv + 2H \rightarrow \equiv Si\text{–}H + \rightarrow \equiv Si\text{–}OH(\Delta Hr$$
$$= -325\ kJ\ mol^{-1}\ at\ 298\ K) \quad [1]$$

Therefore, the H radicals are able to damage low-*k* dielectrics if they have sufficient activation energy required for Reaction 1. Indeed, detailed analysis of the available data shows that the ability of the H_2-based plasma to break Si–CH_3 bonds strongly depends on experimental conditions. According to our study, H radicals formed in downstream H_2 and He/H_2 plasma do not reduce the concentration of Si–CH_3 groups in the temperature range from 20 to 350°C.[23,24] This observation agrees well with the literature data, demonstrating no low-*k* damage in downstream H_2, He/H_2, and He/Ar plasmas.[17,19,20] However, certain additional activation provided, for instance, by ion radiation and UV light makes these reactions possible, causing the difficulty to realize damage-free processes in the reactive ion etching (RIE) condition.[19,25] For instance, Matshushita et al.[19] showed that the damage during the H_2 plasma treatment depends on the type of chamber used. The processes were damage-free in the ion-free discharge. The effect of charged species from H-plasmas for cleaning in the pressure range of 200–400 mTorr was also discussed by Fu et al.[26] The authors compared the H_2 plasma effect on low-*k* with and without plasma leakage reduction (PRL) hardware to reduce the plasma density. They found no Si–CH_3 depletion only when the PRL hardware was used. Similar work and conclusions have also been presented by Lazzeri et al.[22]

The effect of *N* radicals has also been studied in the literature.[17,27] Pure N_2 plasma damages only the top surface of low-*k* materials and makes it hydrophilic. Some nitrogen incorporation and reduction of a Si–CH_3 group in the surface area has also been observed. Our study based on FTIR analysis confirms these observations.[24] The low-*k* film treated with the downstream N_2 plasma shows a small Si–CH_3 bond reduction and a decrease in the water surface contact angle from 95 to 60°. The ability of nitrogen radicals to change surface energy plays a positive role in post-CMP cleaning. The presence of nitrogen radicals remarkably improves the adhesion force of a cleaned stack with the deposited dielectric liner.[28] However, the presence of nitrogen (for instance, in N_2/H_2 plasma) initiates the damage of low-*k* material by hydrogen radicals.[4,17,23]

Effect of NH_x radicals.— One possibility how the NH_3 plasma leads to the film hydrophilization is the replacement of Si–CH_3 bonds by Si–NH_2, which are in turn replaced by Si–OH.[17]

The chemical interaction is represented by the following equations

$$\equiv Si\text{–}CH_3 + NH_2 + H \rightarrow \equiv Si\text{–}NH_2 + CH_4\uparrow$$

$$\equiv Si\text{–}NH_2 + H_2O \rightarrow \equiv Si\text{–}OH + NH_3 \quad [2]$$

Hydrolysis of $\equiv$Si–NH_2 groups was proposed by Posseme et al.[17] Using in situ and ex situ X-ray photoemission spectroscopy analyses, they showed that the nitrogen content in low-*k* films treated in NH_3-RIE plasma has been strongly reduced after air exposure, and the surface became hydrophilic. An additional proof of possibility of hydrolysis is the value of the enthalpy of reaction, $\Delta Hr = -258\ kJ\ mol^{-1}$ at 298 K. This explains the carbon depletion (Fig. 1) and the film hydrophilization (Fig. 7 and 8).

The Si–NH_2 groups on the silica surface might also be formed by the reaction of NH_3 molecules with "highly strained" or ionic siloxane bridges.[29,30] The reaction is represented by the equation

$$\text{Si–O–Si}_{\alpha<144^\circ} + \text{NH}_3 \rightarrow \text{Si–NH}_2 + \text{SiOH} \quad [3]$$

It is also important to analyze the role of NH_x radicals in structural changes occurring in low-*k* dielectrics. We simulated IR Si–O–Si absorbance after the NH_3 plasma exposure.[31] The band related to CH_3 groups shifts to the lower frequencies, which is also evidence of a strong increase in the π-bonding contribution in the Si–O–Si system. Because an increase in the π-bonding causes an increase in the Si–O–Si angle, a pore of 1 nm in radius can increase by 0.4–0.5 Å (that is, by about 2%). This calculation supports the experimental data. We observed an increase in the porosity after the NH_3 plasma treatment of about 1–2% and also a small increase in the pore size. The increased pore size might be also due to the removal of porogen residues by NH_3 plasma (amorphous carbon and cyclic hydrocarbons) embedded in the low-*k* matrix. The porogen residues are generated during the UV curing step of the PECVD low-*k* material. The porogen residues might actively react with the NH_3 plasma radicals and be removed from the low-*k* matrix, which results in the increased pore size.[32]

Effect of He plasma.— In our previous work,[9] we speculated that the major modifications caused by He plasma are due to the energy transfer from EUV photons (He has intense spectral lines below 60 nm) and 2^1S He metastable atoms[33] to the low-*k* structure. The effect of the ion bombardment in a He plasma is not significant because the wafer is placed on the grounded electrode (only self-bias is applied to He ions), and, moreover, the mass of He atoms is relatively small.

The modification of SiO_2 layers caused by EUV radiation from He plasma has been reported.[34,35] EUV light is able to break Si–O bonds on the SiO_2 surface and form so-called "*E′* defects" (oxygen vacancies). Using the absorption coefficients reported by Philipp,[36] one can calculate the penetration depth of EUV photons from He plasma into the silica. These calculations show that the intensity of EUV light with wavelengths of 60–100 nm decreases to $1/e$ within the first 10 nm of silica. Therefore, most photochemical modifications of a silica-based low-*k* film should be restricted to 10–20 nm of the top layer. A more detailed study of the modified layer can be found in our previous work.[9]

We also consider the effect of He metastable atoms on the low-*k* surface. They were reported to cause damage to the porous silica.[37] The typical energies of metastable He atoms are 19.82 eV (2^3S state) and 20.62 eV ($2\ ^1S$ state),[38] which are close to the energies of EUV photons. The high energy metastable atoms could create electron–hole pairs in the film.[38] The holes trapped at the low-*k* film surface form fixed positive charges. The positive charge leads to the Si–O and Si–C bonds scission. The effect of metastable atoms is reported to be localized in the top 1–2 nm of the film.[37]

The defects formed by EUV light and metastable atoms are chemically active and could result in the formation of surface active centers localizing the chemical reactions to the surface. The oxygen vacancies are centers for the chemisorption of active radicals. Another important factor of He plasma pretreatment is a decrease in the size of pore necks.

It is less clear how the He + NH_3 plasma treatment reduces the pore neck size. It was speculated[31] that a rupture of a proton from a CH_3 group also occurs when exposed to He plasma, resulting in a shift of the Si–O–Si bond angles distribution toward larger angles. A subsequent treatment of the film in the NH_3 plasma, after He, promotes cross-linking over these $-CH_x$ groups, as well as Si atoms; $-NH_x$ may serve as a bridge. As a result, the pore size decreases, or the pores get sealed, because the reaction proceeds at the very pore entrance. Because of this, if porosity is measured on the basis of the refractive index, one would not see any essential changes. The number of built-in NH_2 groups may be small because building-in occurs only at the surface; this may be why these groups do not manifest themselves in the IR spectra.

Another factor that might influence the plasma damage reduction is the surface roughening induced by He plasma. The effect of the different He rf power levels on the low-*k* surface roughness was studied by Yanai et. al.[8] They found, using atomic force microscopy, that the mean surface roughness (MSR) was in the range of 0.18–0.39 nm. The as-deposited film showed an MSR of 0.39 nm. With irradiation with He plasma at 100 W, the surface became smoother (MSR = 0.18 nm); when the plasma power was increased to 500 W (MSR = 0.31 nm), the surface became rougher. Yanai et al.[8] presumed that the rougher surface is due to surface carbon depletion at the first monolayer. No correlation between the surface roughness and the damage reduction effect of He plasma was found. The main effect on damage reduction was related to the densified surface by EUV radiation from He plasma. This corresponds with our conclusion that the reduced mean pore size in 10–20 nm of the modified film layer is the most important factor to reduce the depth of radical penetration and therefore the depth of the plasma damage. The mean travel distance of the chemically active radical is significantly reduced due to multiple collisions on narrow pore necks. The multiple collisions significantly increase the probability of recombination or chemisorption of active radicals.

Let us analyze the conclusions stated above on the basis of the Knudsen diffusion mechanism[39] and random walk theory.[40] In our case, the plasma species (radicals and molecules) undergo Knudsen diffusion, traveling into the low-*k* matrix because a mean free path length of species in the NH_3 plasma is a few orders of magnitude larger than the pore size.[39] For instance, assuming a particle size of 2 Å, the mean free path length is approximately 43 μm at 20°C at 530 Pa, while the pore size is approximately 2 nm. The Knudsen diffusion mechanism implies that there are no collisions between the particles in the gas phase. We consider the Knudsen diffusion mechanism for further discussion of a plasma damage model. However, from the viewpoint of the plasma damage, only chemically active species with low-*k* film are important (such as NH_x radicals). To find how the depth of the plasma damage depends on pore size and recombination of active radicals on pore walls, we used the random walk theory formalism.[40] The random walk theory implies that the root-mean-square distance from the origin after a random walk of N steps with length L is $L\sqrt{N}$. So, let us assume that active radicals execute a random walk in the low-*k* skeleton, that in the Nth step, active radicals elastically collide with the pore wall and (*i*) shift an average of 1.5 times of the pore diameter size $L = 1.5d$ or (*ii*) annihilate on the pore wall. The active radical annihilation occurs as a result of its recombination on the pore wall with probability γ_{rec} (i.e., exothermic recombination with another radical on the pore wall; the radical becomes neutral molecule) or chemical reaction with the low-*k* skeleton with probability γ_{chem}, as described in a previous section. Therefore, the total probability of the radical annihilation (total recombination coefficient) is $\gamma = \gamma_{rec} + \gamma_{chem}$. To clarify the link between step number N and γ, let us take three hypothetical recombination coefficients (γ) of NH_3 on the low-*k* pore surface equal to 2×10^{-3}, 2×10^{-2}, and 10^{-2}. In this case, the complete radical recombination on the pore walls occurs after 500, 100, and 50 collisions/steps (N). Therefore, γ is inversely proportional to N. All the discussions above lead us finally to Eq. 4, combining main factors influencing the plasma damage depth (P_d)

$$P_d = ad\sqrt{\frac{1}{\gamma_{rec} + \gamma_{chem}}} \quad [4]$$

According to the proposed model, there are four main factors influencing the P_d. Two factors are related to the pore geometry (a coefficient) (i.e., tortuosity) and the pore size (d). Both influence the mean travel distance $L = a \times d$ ($a = 1.5$) of the chemically active radical. Two other factors are related to the neutralization efficiency of chemically active radicals. The first one is the probability of radical loss in a chemical reaction with the low-*k* matrix (γ_{chem}). The second one is the radical recombination (γ_{rec}) that leads to subsequent creation of the chemically neutral molecule. The recombination coefficients γ_{rec} of N and H radicals on the silica surface at

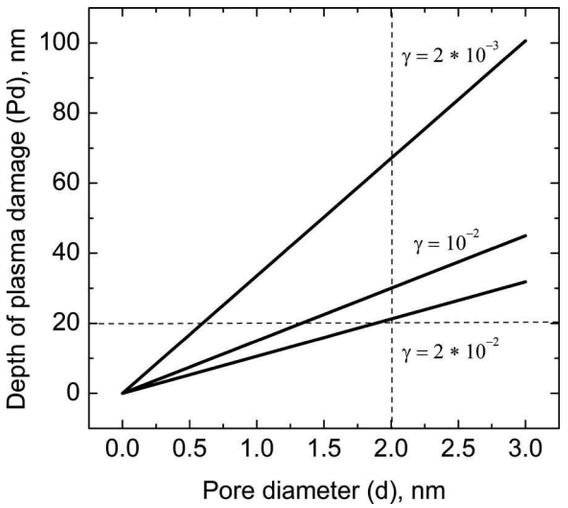

Figure 9. P_ds (for different γ) vs mean pore size of the low-*k* film. Presented data are achieved using Eq. 4, assuming $\gamma = \gamma_{rec} + \gamma_{chem}$ and $a = 1.5$.

350°C are around 1.0×10^{-4}, as reported.[41] The total recombination coefficient (i.e., reaction of O radicals with Si–CH_3 groups or recombination on the Si–O low-*k* skeleton) of active radicals on the ELK HM low-*k* surface has also been studied[42] for O radicals and is 6.0×10^{-3}; and for H radicals, it is 0.22×10^{-3} at 20°C. The literature study shows that γ_{chem} has more impact on plasma damage reduction.

Figure 9 shows the P_ds for different γ plotted using Eq. 4. The P_d increases when (*i*) the pore diameter is larger and (*ii*) the recombination of chemically active radicals on the pore wall is higher. This explains the severe damage during the NH_3 plasma treatment. The pore radius is increased, as discussed in a previous section, and results in increased penetration of the chemically active radicals into low-*k*. The He pretreatment decreases the pore radii and increases the reactivity of NH_x species with low-*k* film. So, the plasma damage is significantly reduced.

Mechanisms of thickness loss of low-k treated in NH_3, He, and sequential He + NH_3 plasmas.— The mechanism of thickness loss in processing plasmas at elevated wafer temperatures (350°C) can be caused by chemical (reactive plasma radicals) and physical plasma effects (UV radiation and hot electrons).[43] Higher thickness loss in the pure NH_3 plasma than in He plasma (Fig. 6) suggests that the chemical effect is domineering. The bond breakage caused by NH_x radicals from the NH_3 plasma occurs within the SiCOH matrix that results in the formation of activated silyl sites. The activated silyl sites are then available to react with other activated silyl species to form Si-Si crosslinks or possibly with SiOH to generate a SiOSi crosslink. [21] The chemical-assisted cross-linkage results in the film thickness loss. The thickness loss in the pure He plasma is much smaller because only the UV and electron-beam and He metastable atoms interact with the film. The effect of UV and metastable atoms is limited to the surface. In the combined He + NH_3 treatment, the thickness loss is prevented due to the reduced penetration depth of NH_3 plasma radicals, which reduces the effect of the chemical-assisted cross-linking.

The thickness loss can also be due to the etching of the dielectric in the studied plasmas. It was proposed by Worsley et al.[3] that the total depth of ash plasma damage is the sum of etch depth and the modification depth. They studied the reducing Ar/H_2 ash plasma in the CCP-type plasma chamber at room temperature, where samples were placed on a biased electrode. Worsley et al.[3] showed that the etch depth increases with the porosity of low-*k* film and the physical sputtering element of etching (ion bombardment). In our case, however, the ion bombardment effect is minimal because films were placed on the grounded electrode. The only possibility to induce film etching would be volatilization of the Si-containing reaction products due to increased temperature of the substrate (350°C). However, only a small fraction of the thickness loss might be due to etching because the reactivity of the NH_3 plasma chemistry with Si–O bonds is very low. Therefore, most of the thickness loss is due to the effect of chemical-assisted cross-linking, as described in the previous paragraph.

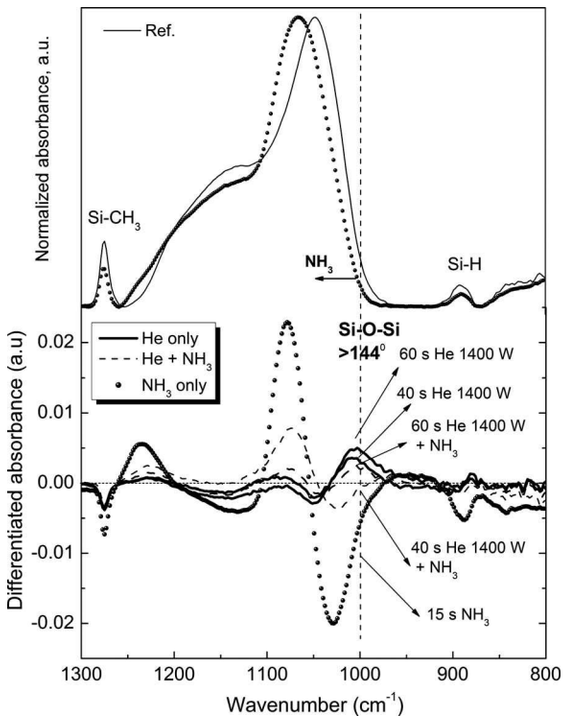

Figure 10. Absorbance and differentiated absorbance for He and NH_3 plasma treatments as measured by FTIR.

Suboxide as a sign of active centers formation.— The peak around 1000 cm^{-1} indicates suboxide or strained ring formation in SiO_2-based materials.[44,45] In this section, we discuss the IR absorbance at 1000 cm^{-1} after studying plasma treatments using the differential FTIR spectroscopy. We presume that the evolution of the 1000 cm^{-1} peak might explain the damage reduction mechanism in the combined He + NH_3 treatment. We propose two possible explanations based on the differential FTIR spectroscopy measurements. The first is that the suboxide appearance after He plasma treatment might indicate an oxygen vacancy formation. The oxygen vacancy might serve as a recombination center for NH_3 plasma radicals. The second possibility is that the NH_3 plasma radicals might react with strained rings, which are mainly formed on the top surface of low-*k* after He plasma treatment (see Eq. 3). Therefore, fewer radicals penetrate the bulk of the low-*k* material. The strained rings play a major role in chemical reactivity and defect formation in porous SiO_2-based materials.[45,46]

Figure 10 shows FTIR spectra of low-*k* film before and after exposure to the various plasmas. The top graph of the figure shows FTIR spectra of the as-deposited and the NH_3-plasma-treated sample in the range of 800–1300 cm^{-1}. The FTIR spectra typical of SiOC:H-type materials contain an absorption band related to the Si–O–Si network (1040–1070 cm^{-1}), a shoulder of a cagelike structure (1100–1150 cm^{-1}), a suboxide absorption band (1000–1030 cm^{-1}), and an absorption band related to Si–CH_3 bonds (1250–1300 cm^{-1}). The SiOC:H film contains bonds local-

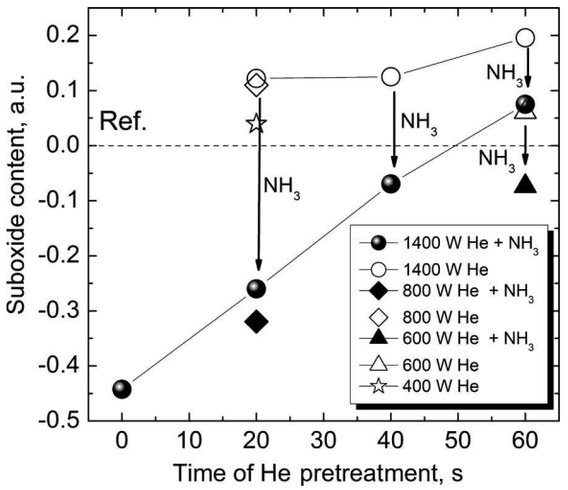

Figure 11. Integrated amplitude of the suboxide peak vs plasma conditions. Arrows indicate the effect of the NH_3 treatment.

ized at 1200 – 1000 cm^{-1} from C–O–C or Si–O–C asymmetric stretching vibrations.[21] However, the identification is difficult because they overlap with the Si–O–Si asymmetric stretching band. After the NH_3 plasma treatment, a clear shift to higher wavenumbers of the Si–O–Si absorption band is observed. This shift is also reflected in the differential spectrum (bottom graph). However, the characteristic changes are much smaller after He plasmas due to the small thickness of the modified layer of 10–20 nm (around 10% of the film thickness). Therefore, we used the differential FTIR to study the changes after successive exposure in He and NH_3 plasmas, as shown in Fig. 10 (bottom graph). The change in absorbance at 1275 cm^{-1} arises from Si–CH_3 groups[47] and decreases the most after the NH_3 plasma treatment.

The peaks of the differential spectra related to Si–O–Si have been reported.[44] The negative peak located close to 1150 cm^{-1} is related to the Si–O–Si (angle ~150°) cagelike structure. The positive peak around 1070 cm^{-1} (angle ~144°) is related to the Si–O–Si network. The highest positive maximum of the network peak appears after pure NH_3 plasma. The peak around 1000 cm^{-1} arises from the Si–O–Si suboxide (angle <144°). This peak appears after He plasma treatment. The amplitude of this peak increases with the time of plasma treatment. The smallest amplitude appears after the successive exposure to He (60 s) and NH_3 (15 s) plasmas. To evaluate the effect of the plasma treatment, the amount of suboxide was estimated by the integration of differentiated absorbance using Eq. 5

$$A_i = \int_{k=1030\ cm^{-1}}^{k=970\ cm^{-1}} A(k)dk \qquad [5]$$

where A_i is the integer of differentiated absorbance and k is the wavenumber. The obtained results are shown in Fig. 11.

One can see that the suboxide is always formed when the pure He plasma is applied (empty symbols). Moreover, the amount of suboxide grows with time and power of He plasma treatment. The suboxide peak disappears when the NH_3 plasma treatment is applied (as indicated by the arrows). The only exception is the 60 s He + 15 s NH_3 plasma treatment when the suboxide peak is still positive, and the film is fully sealed.

Finally, the appearance of the suboxide peak is most probably related to the formation of oxygen vacancies in the low-k film, as was discussed in the previous section. The suboxide peak disappears after their saturation by active radicals (NH_2, H, etc.) from the ammonium plasma. Another possibility is that the NH_3 plasma radicals might react with strained rings formed after He plasma exposure, and this limits their penetration into the bulk of the low-k material (see Eq. 3).

Conclusions

The effect of the combined He and NH_3 plasma treatments on a CVD SiOC:H low-k dielectric is evaluated. The pure NH_3 plasma has a detrimental effect on the low-k material. The NH_3 plasma treatment leads to bulk hydrophilization of the low-k material.

He plasma causes surface modification without damaging the bulk of the low-k. The major modifications caused by He plasma are due to energy transfer from EUV photons and 2^1S He metastable atoms to the low-k structure. The defects formed by EUV light and metastable atoms are oxygen vacancies formed due to the breaking of Si–O bonds, and they are localized in the thin top layer. Oxygen vacancies are centers for chemisorption of active radicals.

The mechanism of plasma damage reduction in the subsequent He + NH_3 plasma treatment is explained on the basis of the Knudsen diffusion mechanism and random walk theory. The defects in low-k structure generated during He plasma treatment traps chemically active radicals on the pore walls. Moreover, He plasma pretreatment decreases the size of pore necks on the surface, which increases the collision frequency of chemically active radicals with the pore walls. The increased collision frequency increases the chance of radical recombination or chemisorption at the first surface monolayers. As a result, He plasma pretreatment makes the low-k material more resistant to the subsequent treatment in the NH_3 plasma. The plasma damage reduction is proportional to He plasma density, which is proportional to rf power during He plasma exposure. Furthermore, the low-k surface is sealed if the He pretreatment exceeds a critical level. The analysis of available literature data suggests that the threshold for plasma sealing in NH_3 and combined He + NH_3 plasmas depends on the type of low-k material and chamber used for the plasma treatment. A possible nature of the sealing capability of NH_3 plasmas might be related to the promoted cross-linking over the $-CH_x$ groups formed in He plasma where $-NH_x$ may serve as a bridge.

Differential FTIR spectroscopy might be used to monitor the pore sealing efficiency in the combined He + NH_3 plasma treatment. The amplitude of absorbance around 1000 cm^{-1} grows with time and power of He plasma treatment. Subsequent NH_3 plasma treatment reduces the 1000 cm^{-1} absorbance. The only exception when the differential 1000 cm^{-1} peak is still positive is when the porous low-k film is fully sealed after the combined He + NH_3 plasma treatment.

Acknowledgments

We acknowledge D. De Roest and H. Sprey, ASM, Belgium for useful discussions and support. A.M.U. acknowledges S. Eslava and C. Huffman for their practical and scientific help.

IMEC assisted in meeting the publication costs of this article.

References

1. K. Maex, M. R. Baklanov, D. Shamiryan, F. Iacopi, S. H. Brongersma, and Z. S. Yanovitskaya, *J. Appl. Phys.*, **93**, 8793 (2003).
2. M. R. Baklanov, A. M. Urbanowicz, G. Mannaert, and S. Vanhaelemeersch, in *International Conference on Solid-State and Integrated Circuit Technology*, Chinese Institute of Electronics, p. 291 (2006).
3. M. A. Worsley, S. F. Bent, S. M. Gates, N. C. M. Fuller, W. Volksen, M. Steen, and T. Dalton, *J. Vac. Sci. Technol. B*, **23**, 395 (2005).
4. A. M. Urbanowicz, A. Humbert, G. Mannaert, Z. Tokei, and M. Baklanov, *Solid State Phenom.*, **134**, 317 (2008).
5. Y. Travaly, J. Van Aelst, V. Truffert, P. Verdonck, T. Dupont, E. Camerotto, O. Richard, H. Bender, C. Kroes, D. De Roest, et al., in *International Interconnect Technology Conference*, IEEE Electron Devices Society, p. 52 (2008).
6. A. Humbert, L. Mage, C. Goldberg, K. Junker, L. Proenca, and J. B. Lhuillier, *Microelectron. Eng.*, **82**, 399 (2005).
7. Y. H. Wang, D. Gui, R. Kumar, and P. D. Foo, *Electrochem. Solid-State Lett.*, **6**, F1 (2003).
8. K. Yanai, T. Hasebe, K. Sumiya, S. Oguni, and K. Koga, *MRS Bull.*, **863**, B2.3 (2005).
9. A. M. Urbanowicz, M. R. Baklanov, J. Heijlen, Y. Travaly, and A. Cockburn,

Electrochem. Solid-State Lett., **10**, G76 (2007).
10. P. Verdonck, D. De Roest, S. Kaneko, R. Caluwaerts, N. Tsuji, K. Matsushita, N. Kemeling, Y. Travaly, H. Sprey, M. Schaekers, et al., *Surf. Coat. Technol.*, **201**, 9264 (2007).
11. M. R. Baklanov, K. P. Mogilnikov, V. G. Polovinkin, and F. N. Dultsev, *J. Vac. Sci. Technol. B*, **18**, 1385 (2000).
12. M. R. Baklanov and K. P. Mogilnikov, *Microelectron. Eng.*, **64**, 335 (2002).
13. D. Shamiryan, M. R. Baklanov, and K. Maex, *J. Vac. Sci. Technol. B*, **21**, 220 (2003).
14. W. Puyrenier, V. Rouessac, L. Broussous, D. Rebiscoul, and A. Ayral, *Microporous Mesoporous Mater.*, **106**, 40 (2007).
15. D. Rebiscoul, L. Broussous, W. Puyrenier, V. Rouessac, and A. Ayral, *J. Phys.: Conf. Ser.*, **152**, 012002 (2009).
16. M. R. Baklanov, K. P. Mogilnikov, and T. Q. Le, *Microelectron. Eng.*, **83**, 2287 (2006).
17. N. Posseme, T. Chevolleau, T. David, M. Darnon, O. Louveau, and O. Joubert, *J. Vac. Sci. Technol. B*, **25**, 1928 (2007).
18. H. G. Peng, D. Z. Chi, W. D. Wang, J. H. Li, K. Y. Zeng, R. S. Vallery, W. E. Frieze, M. A. Skalsey, D. W. Gidley, and A. F. Yee, *J. Electrochem. Soc.*, **154**, G85 (2007).
19. A. Matshushita, N. Ohashi, K. Inukai, H. J. Shin, S. Sone, K. Sudou, K. Misawa, I. Matsumoto, and N. Kobayashi, in *International Interconnect Technology Conference*, IEEE Electron Devices Society, p. 147 (2003).
20. I. L. Berry, Q. Han, C. Waldfried, O. Escorcia, and A. Becknell, in *Semiconductor Equipment and Materials International: Technical Symposium: Innovations in Semiconductor Manufacturing*, Semiconductor Equipment and Materials International (2004).
21. A. Grill, V. Sternhagen, D. Neumayer, and V. Patel, *J. Appl. Phys.*, **98**, 074502 (2005).
22. P. Lazzeri, G. J. Stueber, G. S. Oehrlein, R. McGowan, and E. Busch, *J. Vac. Sci. Technol. B*, **24**, 2695 (2006).
23. A. M. Urbanowicz, D. Shamiryan, P. Marsik, Y. Travaly, A. Jonas, P. Verdonck, K. Vanstreels, A. Ferchichi, D. De Roest, H. Sprey, K. Matshushita, S. Kaneko, N. Tsuji, S. Luo, O. Escorcia, I. L. Berry, C. Waldfried, S. De Gendt, and M. R. Baklanov, in *Advanced Methalization Conference*, UC Berkley, p. 594, San Diego (2009).
24. A. Urbanowicz, D. Shamiryan, B. Chen, P. Verdonck, and M. Baklanov, *Characterization of Low-k Dielectric Damage during Downstream Plasma Strip at Elevated Temperature*, IMEC, Leuven (2008).
25. I. L. Berry, Q. Han, C. Waldfried, O. Escorcia, and A. Becknell, in *SEMI Technical Symposium: Innovations in Semiconductor Manufacturing*, SEMICON WEST (2004).
26. X. Fu, J. Forester, J. Yu, P. Gopalraja, S. Ahn, A. Demos, and P. Ho, *IEEE*, 51 (2006).
27. S. L. Xu, C. Qin, L. Diao, D. Gilbert, L. Hou, A. Wiesnoski, E. Busch, R. McGowan, B. White, and F. Weber, *J. Vac. Sci. Technol. B*, **25**, 156 (2007).
28. P. Verdonck, *Influence of Reductive Plasmas on Adhesion of Dielectric Liner with Cleaned Stacks*, IMEC, Leuven (2008).
29. J. B. Peri, *J. Phys. Chem.*, **70**, 2937 (1966).
30. G. A. Blomfield and L. H. Little, *Can. J. Chem.*, **51**, 1771 (1973).
31. F. N. Dultsev, A. M. Urbanowicz, and M. R. Baklanov, in *Material Research Society Proceedings*, Material Research Society (2008).
32. A. M. Urbanowicz, K. Vanstreels, D. Shamiryan, S. De Gendt, and M. Baklanov, *Electrochem. Solid-State Lett.*, **12**, H292 (2009).
33. R. S. Van Dyck, H. A. Shugart, and C. E. Johnson, *Phys. Rev. A*, **5**, 991 (1972).
34. K. Yokogawa, Y. Yajima, T. Mizutani, S. Nishimatsu, and K. Suzuki, *Jpn. J. Appl. Phys., Part 1*, **29**, 2265 (1990).
35. T. Tatsumi, S. Fukuda, and S. Kadomura, *Jpn. J. Appl. Phys., Part 1*, **33**, 2175 (1994).
36. H. R. Philipp, in *Handbook of Optical Constants of Solids*, E. D. Palik, Editor, p. 749, Academic, Orlando (1985).
37. K. Kurihara, T. Ono, K. Kohmura, H. Tanaka, N. Fujii, N. Hata, and T. Kikkawa, *J. Appl. Phys.*, **101**, 113301 (2007).
38. T. Ono, N. Itabashi, I. Ochiai, S. Yamamoto, and K. Mochiji, *Jpn. J. Appl. Phys., Part 1*, **36**, 6718 (1997).
39. C. K. Ho and S. W. Webb, *Gas Transport in Porous Media*, pp. 12–13, Springer, Berlin (2006).
40. G. H. Weiss, *Aspects and Applications of The Random Walk*, pp. 1–5, North-Holland, Amsterdam (1994).
41. Y. C. Kim and M. Boudart, *Langmuir*, **7**, 2999 (1991).
42. O. V. Braginsky, A. S. Kovalev, D. V. Lopaev, E. M. Malykhin, T. V. Rakhimova, A. N. Vasilieva, S. M. Zyryanov, and M. R. Baklanov, *IEEE Trans. Plasma Sci.* **37**, 1697 (2009).
43. V. Jousseaume, A. Zenasni, L. Favennec, G. Gerbaud, M. Bardet, J. P. Simon, and A. Humbert, *J. Electrochem. Soc.*, **154**, G103 (2007).
44. A. Grill and D. A. Neumayer, *J. Appl. Phys.*, **94**, 6697 (2003).
45. D. R. Hamann, *Phys. Rev. B*, **55**, 14784 (1997).
46. H. Hosono, Y. Ikuta, T. Kinoshita, K. Kajihara, and M. Hirano, *Phys. Rev. Lett.*, **87**, 175501 (2001).
47. T. R. Crompton, *The Chemistry of Organic Silicon Compound*, p. 416, John Wiley & Sons, New York (1989).